

Design of Model Reference Controller of Variable Speed Wind Generators for Frequency Regulation Contribution

Elvisa Becirovic
Elektroprivreda BiH
Sarajevo, Bosnia and Herzegovina

Jakub Osmic, Mirza Kusljagic
Faculty of Electrical Engineering
Tuzla, Bosnia and Herzegovina

Nedjeljko Peric
Faculty of Electrical Engineering and Computing
Zagreb, Croatia

Received: January 27, 2021. Revised: March 15, 2021. Accepted: March 16, 2021. Published: March 22, 2021.

Abstract—This paper presents a novel control algorithm for variable speed wind generators (VSWG), designed to provide support to grid frequency regulation. The proposed control algorithm ensures that VSWG “truly” emulates response of a conventional generating unit with non-reheat steam turbine (GUNRST) in the first several seconds after active power unbalance. A systematic method of analysis and synthesis of the new control algorithm is described in detail.

Keywords— variable speed wind generator; primary frequency control; emulation of inertial response; droop control; model reference controller; design methodology

I. INTRODUCTION

DUE to the increasing ratio of variable speed wind generators (VSWG) penetration in electrical power generation there is a need for their contribution to grid frequency regulation. Since VSWG operates at maximum power point tracking (MPPT) and uses AC/DC/AC converter, there is no direct coupling between grid frequency deviation and its active power generation. A control algorithm for VSWG, which will ensure its participation in grid frequency regulation, should ensure extraction of additional electric power from VSWG during frequency disturbance.

The steady state of electrical power system (EPS) is characterized by balance between active power generation and active power consumption. Following a sudden active power disturbance in EPS, such as loss of generating unit or sudden increase in active power load, the rest of EPS cannot respond immediately by increasing necessary (missing) turbine mechanical power. This is due to nonzero time constants of governor and turbine dynamics. As a result the grid frequency starts to decrease. Active power balance is first established from electromagnetic energy accumulated in the system immediately after disturbance occurrence. Then, provided EPS transient stability is maintained, in the so called inertial phase of rotating machines frequency response, kinetic energy is converted to active power and delivered to the rest of the

system to maintain active power balance. The inertial phase lasts no more than several seconds. In this phase the turbine also starts to deliver additional power to the generator. Provided frequency stability is maintained, this action results in decrease and eventual halting of frequency declining and consequently in recovery of rotating machines rotation speed and kinetic energy. Finally, after approximately 30 seconds, frequency of the system stabilizes at the new steady state value. The permitted interval of the grid frequency change is quite short, so the system of turbine mechanical power regulation must be fast enough to prevent frequency deviation below the limited level in order to avoid frequency disturbance propagation, which can eventually lead to frequency instability.

The main indices describing grid frequency behaviour following active power disturbance are: rate of change of frequency (ROCOF), minimal value of frequency reached (frequency nadir) and steady state frequency deviation (SSFD). The value of ROCOF mainly depends on the sum of moments of inertia of rotating machines. By increasing EPS moment of inertia, ROCOF decreases. Frequency nadir is determined by: intensity of power disturbance, kinetic energy stored in EPS, number of generators contributing primary frequency control and dynamic characteristics of generators, loads, and governors. The SSFD value is determined by speed governor droop characteristics of generating units participating in primary frequency control.

Characteristic responses of mechanical power and turbine speed of three conventional generating units: unit with a reheat steam turbine (dashed line), generating unit with a non-reheat steam turbine (GUNRST) (solid line) and hydraulic unit (dash dotted line), to a unit step change in active load are presented in Fig. 1 and Fig. 2 [1]. Figures indicate that GUNRST has the fastest response. Hydraulic unit has the slowest response, since it has a non-minimum phase transfer function (unstable zero in the transfer function).

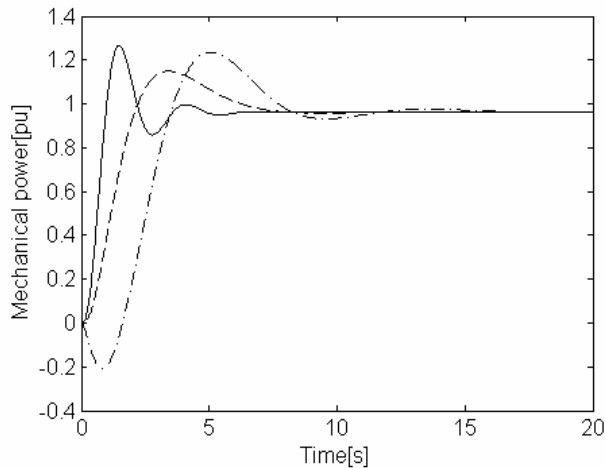


Fig. 1. Deviation of generating units mechanical power to a unit step increase in load demand: generating unit with a non-reheat steam turbine (solid line), generating unit with a reheat steam turbine (dashed line), hydraulic unit (dash dotted line).

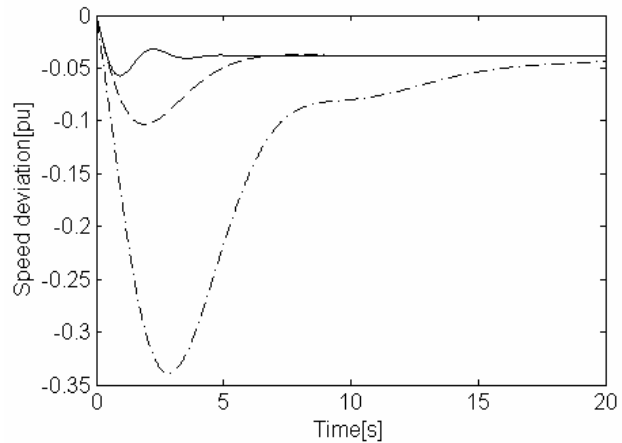


Fig. 2. Speed deviation of generating units to unit step increase in active load demand: generating unit with a non reheat steam turbine (solid line), generating unit with a reheat steam turbine (dashed line), hydraulic unit (dash dotted line).

Nowadays, the most used types of large power wind generators are VSWG, such as double fed induction generators (DFIG) and fully rated converter wind turbine (FRCWT) [2]. Since DFIG and FRCWT use fast electronic converters (AC/DC/AC) and operate at MPPT, there is no (or very little) direct coupling between grid frequency deviation and their active power generation. Operation at MPPT results in VSWG having no spinning reserve, which could be used to support frequency regulation after disturbance. It is, therefore, necessary to modify VSWG control algorithms to support grid frequency regulation. DFIG and FRCWT frequency regulation capabilities have been in focus of interest of scientific community over past years [2]-[11]. As a result, a number of papers have been published, dealing with different control algorithms for VSWG, designed to provide contribution to primary frequency control [12]. These control algorithms can be classified into: inertial control, droop control, deloading control or their combination [3]-[5], [7] and [10]. All above mentioned approaches pertain to VSWG control level. Control algorithms for control coordination of the wind farm level or EPS as a whole, such as in [8] and [11], are also proposed.

Inertial control approach enables transformation of the part of VSWG kinetic energy into electrical power, which is instantaneously delivered to EPS by fast electronic converter. Time constant of electronic converter is of milliseconds order. Transformation of kinetic energy to electric power causes VSWG speed decrease, which must be limited in order to prevent speed of turbine reaching its minimum permitted level. In addition, since VSWG traditionally operate at MPPT, wind generator speed must be recovered to this optimum value as soon as possible. Since VSWG have no spinning reserve, speed recovery is performed by VSWG delivering less active power than optimum. This ensures speed of VSWG being recovered to its optimum value (for constant wind speed to the value before the frequency transient).

The main challenge in inertial (and droop) control of VSWG approaches is “shaping up” the responses of active power delivered to the rest of EPS and the responses of

VSWG speed after grid frequency disturbance. A number of different inertial controllers, droop controllers or their combinations have been proposed, i.e. as presented in [3]-[5], [7], [10] and [11]. The main idea, presented in these approaches, is the following: add a new control signal C_{ad} to the existing torque control loop, before or after PI controller, which will force VSWG to emulate inertial behaviour or inertial behaviour plus droop control of conventional generators, following a grid frequency disturbance. Then, such combined signal appears as reference torque input T_{ref} to electronic converter, such as in [4], or as reference active power input P_{ref} such as in [7]. These approaches are illustrated in Fig. 3. In the referred research for inertia emulation the so called washout filter is used for inertial signal zeroing at network frequency steady state as well as for grid frequency (or frequency deviation) signal filtering. A washout filter in fact performs an ideal derivation or filtered derivation of the grid frequency (or frequency deviation) signal. In some papers additional compensator block is used to create phase compensation of signal leaving washout filter [3].

If signal C_{ad} is added after PI controller, then torque control loop considers this signal as disturbance signal. In this case it is not necessary to derive grid frequency signal since integral part of PI controller makes this signal of no effect at steady state, even if steady state value of $\Delta\omega$ is different from zero. Droop part of additional signal C_{ad} in Fig. 3 is used to emulate droop behaviour of conventional regulator in primary frequency control.

A lack of analytical methods for analysis and synthesis of VSWG inertial and/or droop control are evident, i.e. in [2], [3], [4], [7] and [11]. Accordingly, in these references the parameters of inertial and droop controllers were mainly determined by “trial and error method”. In addition, the following question: “What should a “desirable” response of active power injected by VSWG into the EPS after an active power disturbance look like?” has not been answered yet. VSWG’s rotational speed after supporting grid frequency

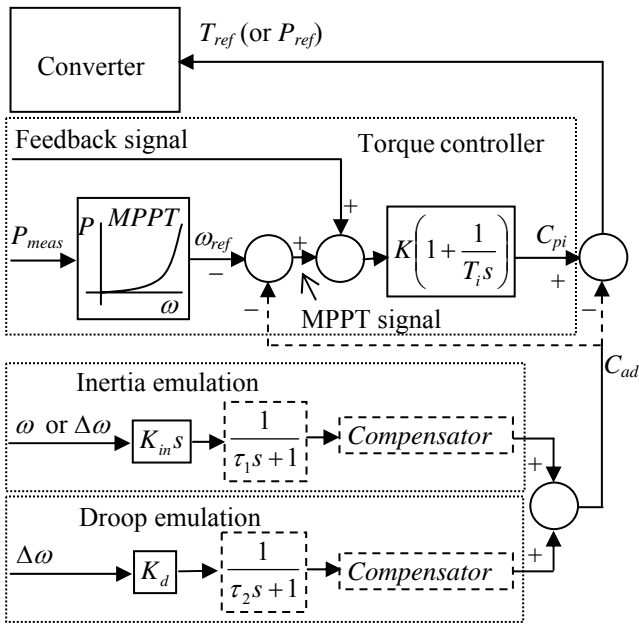


Fig. 3. Control loops for wind unit active power with inertia and droop emulation. P_{meas} – measured active power of wind unit, ω - grid frequency, $\Delta\omega$ - grid frequency deviation, C_{pi} – control signal from PI controller, C_{ad} – additional control signal for inertia and droop emulation.

must recover to the optimal, pre-disturbance value. Hence the same amount of VSWG kinetic energy that was delivered to the EPS after active power disturbance must be supplied to VSWG in the process of recovering its speed. Consequently, if VSWG delivered kinetic energy is too large in inertial phase, than VSWG delivers much less power than before the disturbance during VSWG speed recovery phase. This will be regarded by EPS as the new active power disturbance before reaching the new grid frequency steady state. Thus response of VSWG delivered active power during entire frequency transient is very important. Some authors suggest that process of VSWG speed recovery should be performed smoothly by using “smooth” control algorithm, whereas others propose performing switching off VSWG frequency support at different time [4], [7] and [8]. A novel VSWG control algorithm designed to support frequency regulation is proposed in this paper. Block diagram of proposed control algorithm is presented in Fig.4. Main characteristics of the proposed control algorithm (controller) are the following:

- Analytical design method of VSWG controller supporting grid frequency regulation, following active power disturbance, has been presented. By using the new control algorithm, VSWG “truly” emulates reference GUNRST model in several seconds after frequency disturbance. Reference generating unit can be any existing GUNRST or a hypothetical GUNRST with values of nominal power and inertia constant equal (or close) to those of the controlled wind turbine.
- Since MPPT control loop uses PI controller which cancels nonzero stationary value of signal C_{ad} , in the new control algorithm frequency (deviation) derivation is not used. Instead, a lead compensator is used in the new control algorithm.

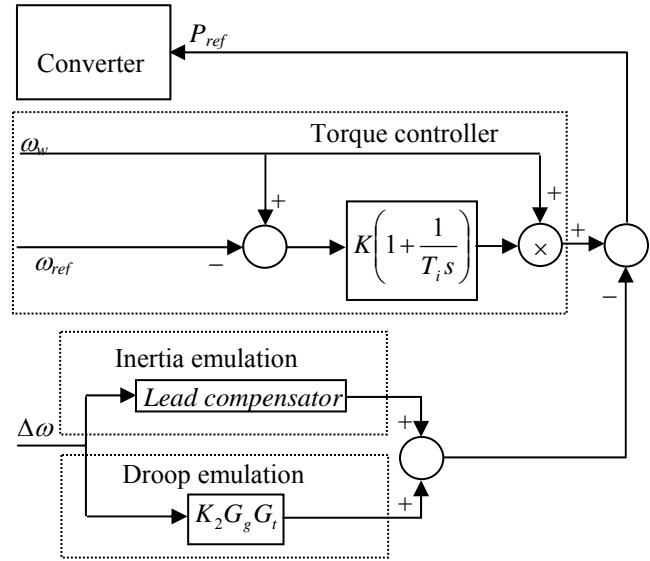


Fig. 4. Proposed controller of VSWG active power with inertia and droop emulation

II. MODELS OF GENERATING UNITS USED IN FREQUENCY STABILITY STUDIES

A simplified generic block diagram of conventional generating unit is presented in Fig. 5. By variation of its parameters, from this block diagram, it is possible to simulate dynamic response of any conventional generating unit (including GUNRST) participating in primary frequency control [1]. In Fig. 5 G_g is governor transfer function, G_{tdc} is transfer function of transient droop compensation block - which exists only in hydraulic generating unit, G_t is turbine transfer function, H is inertia constant of rotating parts of generating unit, R is droop constant, and D models variation of load with grid frequency variation. Inertia constants of conventional generators are in 2-9 s range [13]. Typical inertia constants of wind generators are in 2-6 s range [14]. A typical frequency response to a step of load increase ΔP_e at time $t = 1$ s is presented in Fig. 6. Neglecting the effect of load variation ($D = 0$) from Fig. 5 it can be seen that

$$\Delta P_e = \Delta P_m - \Delta P_a, \quad (1)$$

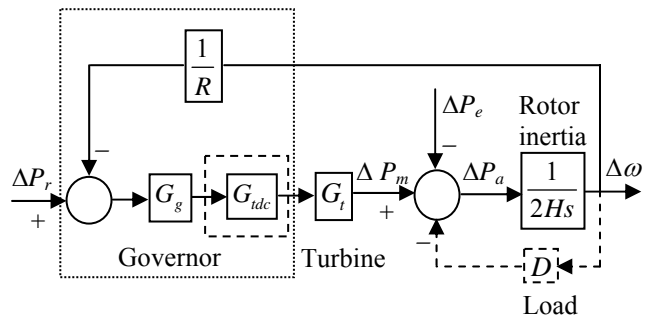


Fig. 5. Generic block diagram of conventional power unit used in frequency stability studies.

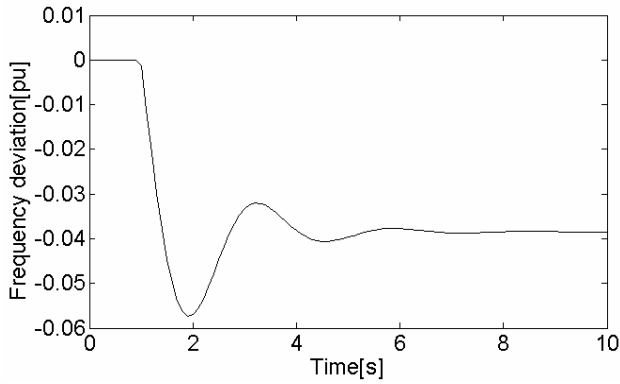


Fig. 6. Frequency response to a unit step of active power disturbance.

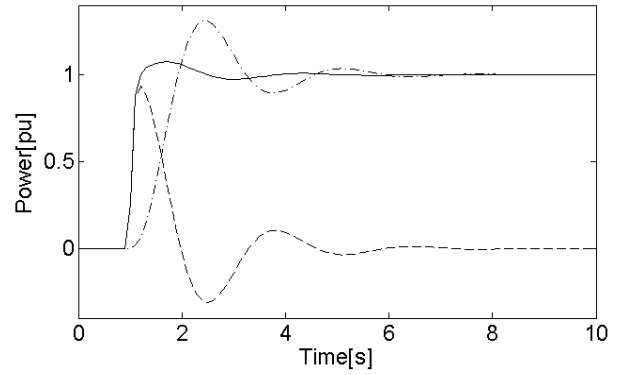


Fig. 7. Inertial power (dashed line), mechanical power (dash dotted line) and electrical power (solid line).

where ΔP_e is electrical power of generating unit, $\Delta P_m = -\frac{1}{R}G_g G_t \Delta \omega$ is turbine mechanical power, and $\Delta P_a = 2Hs \Delta \omega$ is accelerating (inertial) power. Accordingly, ΔP_e can be expressed as

$$\Delta P_e = -2Hs \Delta \omega - \frac{1}{R}G_g G_t \Delta \omega. \quad (2)$$

In case that model of generating unit is known, it is possible to determine (approximate) active power disturbance by using (2) and by measuring $\Delta \omega$. In (2), however, an ideal derivation of frequency deviation is performed. An ideal derivation of signal cannot be achieved. The term in (2) should be replaced by filtered derivation of frequency deviation. According to this, the expression for approximation of electrical power is

$$\begin{aligned} \Delta P_e &= -\frac{2Hs}{\tau_B s + 1} \Delta \omega - \frac{1}{R}G_g G_t \Delta \omega \\ &= -\frac{2Hs}{\frac{s}{\omega_B} + 1} \Delta \omega - \frac{1}{R}G_g G_t \Delta \omega = -G_i \Delta \omega - G_m \Delta \omega \end{aligned} \quad (3)$$

where τ_B is time constant of the first order time lag (low pass filter) $\frac{1}{\tau_B s + 1}$, and $\omega_B = 1/\tau_B$ is its bandwidth. The

bandwidth ω_B should be large enough to preserve useful information in signal $\Delta \omega$. At the same time, the bandwidth must be limited from above to filter noise present in $\Delta \omega$. Considering frequency spectrum of signal from Fig. 6 it can be concluded that an upper bound of $\Delta \omega$ frequency spectrum could be chosen as $\omega_B = 15 \frac{rad}{s} (\approx 2.5 \cdot 2\pi)$ or even lower.

This value can be changed depending on characteristics of considered EPS. By performing frequency measurement and using (3) it is possible to determinate (approximate) active power disturbance as presented in Fig. 7. It is clear from Fig. 7 that quite good active power disturbance (unit step of active load demand at time $t = 1$ s) approximation is achieved. The increase of ω_B is followed by the increase of approximation accuracy. The same figure shows that inertial power time

constant is much lower than mechanical power time constant. Accordingly, in the first moments after frequency disturbance, the missing active power in EPS is almost completely generated due to decreasing kinetic energy of rotating machines.

III. A NOVEL APPROACH OF VSWG CONTROL FOR FREQUENCY REGULATION

A novel approach to control VSWG electrical power in order to support grid frequency regulation during transient process after a sudden active power disturbance is presented in this paper. The basic idea is to force VSWG to behave as close as possible to reference GUNRST within few seconds (0 ÷ 5 seconds) after frequency disturbance. This approach ensures that during the initial phase of frequency transients EPS with VSWG behaves exactly as EPS with GUNRST connected at same point as VSWG. For the purpose of analysis and synthesis simplification, this paper assumes that reference GUNRST has the same inertia constant and nominal active power as VSWG.

Since VSWG that operates at MPPT have no spinning reserve, it is not possible to exactly realize the control law given by (3). The first term in (3) (inertial power) converge to zero as time goes to infinity since it includes s in its numerator. The second term in (3) converges to $1/R [dcgain(G_g G_t) \Delta \omega_{ss}]$ as time goes to infinity, where $\Delta \omega_{ss}$ is steady state frequency deviation. If $dcgain(G_g G_t) = 1$ then steady state of the second term in (3) converges to $\Delta \omega_{ss}/R$. To solve this problem a term that has the same static gain as term $\frac{1}{R}G_g G_t \Delta \omega$ is added to the right hand side of (3). This term should not significantly change behaviour of (3) in frequency transient process but it must force right hand side of (3) to converge to zero with a desirable time constant τ as time increases to infinity. The following additional term is proposed in this paper

$$G_{ad} = \frac{1/R}{(\tau s + 1)} G_g G_t. \quad (4)$$

Accordingly, the new control law becomes

$$\begin{aligned} \Delta P_{e1} &= -\frac{2Hs}{\tau_B s + 1} \Delta\omega - \frac{1}{R} G_g G_t \Delta\omega + \frac{1/R}{(\tau s + 1)} G_g G_t \Delta\omega \\ &= -\frac{2Hs}{\tau_B s + 1} \Delta\omega - \frac{1}{R} \frac{\tau s}{\tau s + 1} G_g G_t \Delta\omega \\ &= -s \left(\frac{2H}{\tau_B s + 1} - \frac{1}{R} \frac{\tau}{\tau s + 1} G_g G_t \right) \Delta\omega = -G_t \Delta\omega - G_{mm} \Delta\omega. \end{aligned} \quad (5)$$

Equation (5) indicates that second term G_{mm} of the proposed control law also converges to zero since it has s in its numerator. The second term G_{mm} in (5) differs from the second term G_m in (3) in the dipole

$$G_d = \frac{\tau s}{\tau s + 1}. \quad (6)$$

This dipole has the pole $s_p = -1/\tau$. If τ is chosen as sufficiently large positive number then the pole of dipole (6) is very close to its zero $s_z = 0$. Multiplication of a transfer function with a dipole slightly changes the response of the transfer function in transient process. At the same time, the behaviour of a transfer function at steady state can be substantially changed. The responses of G_m and G_{mm} to a unit step signal are presented in Fig. 8.

The transfer functions of governor and turbine are chosen as

$$G_g = \frac{1}{(\tau_g s + 1)}, \quad G_t = \frac{1}{(\tau_t s + 1)}. \quad (7)$$

The simulation is performed with time constant of governor $\tau_g = 0.2$, turbine time constant $\tau_t = 0.3$, and droop constant $R = 0.04$ [1]. As expected duration of overall transient process in EPS is about 30 seconds it follows that appropriate value of the time constant τ is $\tau = 30 - \tau_g - \tau_t = 30 - 0.2 - 0.3 = 29.5$. Fig. 8 shows that there is little difference between responses G_m and G_{mm} within first several seconds. This was the ultimate goal of the second term modification in control law (3).

A published block diagram of DFIG that operates at MPPT is shown in Fig. 10 [6], [15], [16], and [17]. A similar control structure is used for FRCWT [18]. This model today is known as generic model of VSWG active power control [17]. Block diagram in Fig. 9 is nonlinear which complicates its analysis and synthesis. A method for linearization of the block diagram shown in the Fig. 9 is presented below.

A typical value of time constant T_{con} is 0.02 seconds (such

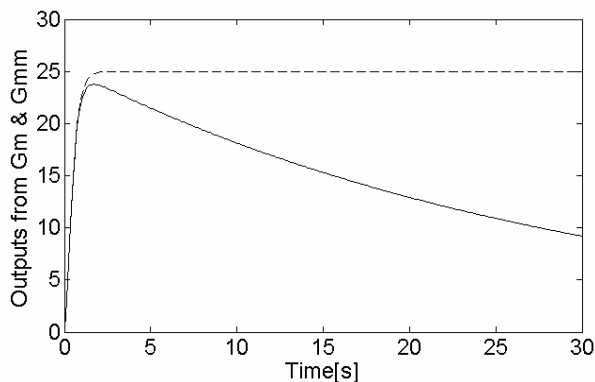


Fig. 8. Step response of G_m (dashed line) and G_{mm} (solid line)

as in [6]). In comparison to time duration of frequency transient process this time constant can be neglected. In order to get linear model corresponding limiter is neglected as well. A typical value of time constant T_f is 60 seconds (such as in [17]). This is the reason that for purposes of synthesis of controller (not in the simulation) reference rotational speed of VSWG - ω_{ref} can be kept constant during entire frequency transient process. Considering all above mentioned, a simplified block diagram of VSWG control system, presented in Fig. 9, is shown in Fig. 10. In Fig. 10 ω_{ref0} represents the optimal VSWG rotational speed before frequency disturbance. This block diagram is still non linear, due to existence of signal multiplication and division. VSWG operate at the MPPT, thus at pre-disturbance steady state VSWG speed is optimal. At the vicinity of the optimal VSWG speed, characteristic tip speed ratio (λ) - captured mechanical power (P_m) is somewhat flat in comparison to other regions of this characteristic. Since frequency transient process is relatively short, it is expected that wind speed will not considerably change during this process. Consequently, captured mechanical power of VSWG can be regarded as constant during frequency transient process. If too large variation of VSWG speed is not expected, then, for analysis and synthesis purposes, VSWG speed signal entering block of multiplication and division can be regarded as constant that is $\omega_w = \omega_{ref0} = const$. If instead of signals their variations around equilibrium point are considered then linear model of the system, presented in Fig. 11, could be developed. A new control signal is added after multiplication of the signal leaving PI controller by actual wind speed. The block with transfer function G_1 in Fig. 11 represents the novel control algorithm. The input in this block is grid frequency deviation $\Delta\omega$. In order to simplify further analysis it is assumed that $H_w = H$.

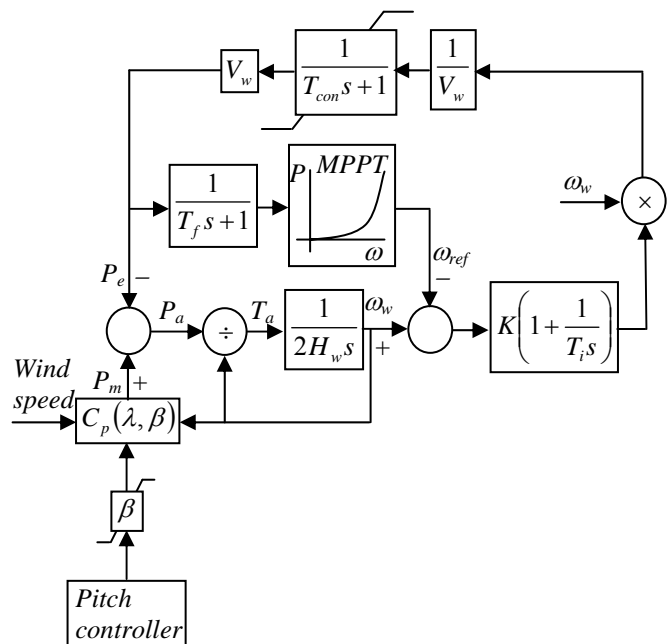


Fig. 9. Block diagram of control system of VSWG (adopted from [6], [15], [16], and [17]).

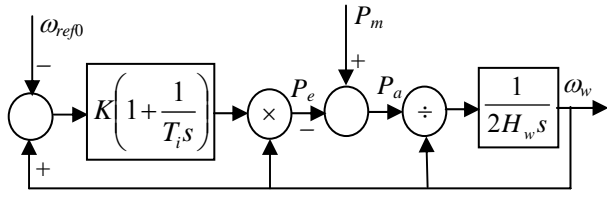


Fig. 10. Simplified block diagram of control system of VSWG.

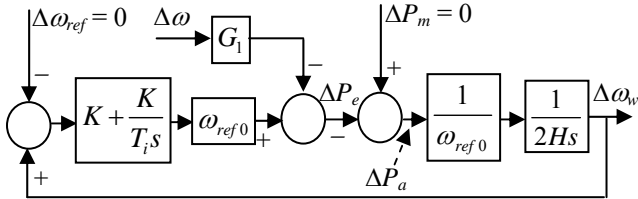


Fig. 11. Linearized control structure of VSWG for frequency control support from Fig. 10.

Fig. 11 shows that electrical power being injected by VSWG to EPS after frequency disturbance is given by

$$\Delta P_e = -\Delta P_a. \quad (8)$$

Transfer function G_1 from Fig. 11 should be chosen in the way that injected electrical power ΔP_e conforms to control law (5). In Fig. 11 symbol $\Delta\omega$ represents deviation of grid frequency.

Transfer function from $\Delta\omega$ to ΔP_e is defined as

$$\frac{\Delta P_e}{\Delta\omega} = -\frac{G_1}{\Delta}, \quad (9)$$

where Δ represents characteristic function of the system and it is given by

$$\Delta = 1 + K \left(1 + \frac{1}{T_i s} \right) \omega_{ref0} \frac{1}{\omega_{ref0}} \frac{1}{2Hs} = \frac{2Hs^2 + Ks + \frac{K}{T_i}}{2Hs^2}. \quad (10)$$

Substituting (10) into (9) gives

$$\begin{aligned} \frac{\Delta P_e}{\Delta\omega} &= -\frac{\Delta P_a}{\Delta\omega} = -\frac{G_1}{\Delta} = -\frac{2Hs^2 G_1}{2Hs^2 + Ks + \frac{K}{T_i}} \\ &= -\frac{s^2 G_1}{s^2 + \frac{K}{2H}s + \frac{K}{2HT_i}}. \end{aligned} \quad (11)$$

The poles of transfer function (11) are

$$\Delta_{1/2} = -\frac{K}{4H} \pm \frac{1}{2} \sqrt{\left(\frac{K}{2H} \right)^2 - \frac{4K}{2HT_i}}. \quad (12)$$

If request of VSWG control system is that the fastest response to a step of $\Delta\omega_{ref}$ without overshoot is achieved, then parameters K and T_i of PI controller should be chosen so that poles (12) are real, negative and equal (the transfer function (11) must have double negative pole).

The pole of the transfer function (11) is double and equals to

$$\Delta_{1/2} = -\frac{K}{4H}, \quad (13)$$

if the following equation is valid

$$T_i = \frac{4K}{2H} \cdot \left(\frac{2H}{K} \right)^2 = \frac{8H}{K}. \quad (14)$$

Due to integral part of PI controller, VSWG speed equals to reference speed in steady state. From (11) it follows

$$\Delta P_e = -\frac{s^2 G_1}{s^2 + \frac{K}{2H}s + \frac{K}{2HT_i}} \Delta\omega = -\frac{s^2 G_1}{\left(s + \frac{K}{4H} \right)^2} \Delta\omega. \quad (15)$$

In addition from Fig. 11

$$\begin{aligned} \Delta\omega_w &= \frac{1}{\omega_{ref0}} \frac{1}{2Hs} \frac{G_1}{\Delta} \Delta\omega \\ &= \frac{1}{2H\omega_{ref0}} \cdot \frac{s G_1}{s^2 + \frac{K}{2H}s + \frac{K}{2HT_i}} \Delta\omega. \end{aligned} \quad (16)$$

From (16) it follows that there is an inverse proportionality between VSWG speed deviation $\Delta\omega_w$ and initial wind speed ω_{ref0} . From (15) it follows that ΔP_e in steady state diminishes due to existence of term s^2 in the numerator of transfer function. In addition, $\Delta\omega_w$ also goes to zero as time passes if there is no pole of G_1 at the origin of s plane (that is there is no s in denominator of G_1). This is due to existence of s in the numerator of expression at the right hand side of (16). This way it is ensured that VSWG speed and electrical power of VSWG at steady state restore to values before frequency disturbance. At the end of transient process, steady state frequency deviation becomes $\Delta\omega_{ss}$. From above considerations we can also conclude that, in order to achieve specified goals, the existence of term s (ideal derivation) in numerator of G_1 is unnecessary. This is qualitatively new fact in comparison to published papers, since they present transfer function of controller including s in its numerator [4], [5], [7], [9] and [11].

In order to achieve that VSWG emulates reference-GUNRST model it is necessary that expression on the right hand side of (15) equals expression on the right hand side of (5). This could be achieved only if G_1 includes integrator $1/s$. In this case, however, according to previous considerations, VSWG speed will not be restored to the value before frequency disturbance. Because of this it is necessary to make modification of the reference model (5). This can be performed by multiplying transfer function of the reference model with a dipole that includes s in its numerator, without affecting reference model (5) during transient process. Then, the new reference model is

$$\begin{aligned} \Delta P_{e2} &= \frac{\tau_1 s}{\tau_1 s + 1} \left(-\frac{2Hs}{\tau_B s + 1} - \frac{1}{R} \frac{\tau}{\tau s + 1} G_g G_t \right) \Delta\omega \\ &= \frac{\tau_1 s^2}{\tau_1 s + 1} G_r \Delta\omega \end{aligned} \quad (17)$$

$$\text{where } G_r = -\frac{2H}{\tau_B s + 1} - \frac{1}{R} \frac{\tau}{\tau s + 1} G_g G_t.$$

Time constant τ_1 should be selected big enough to prevent

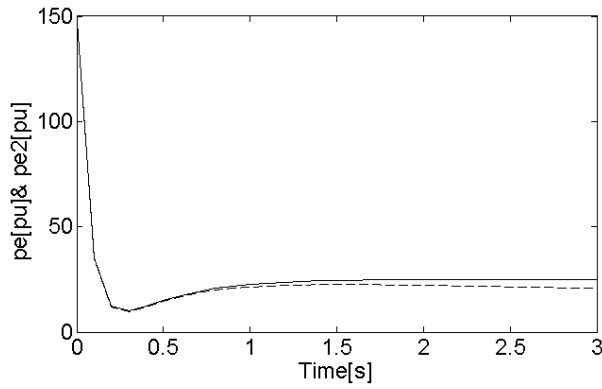


Fig. 12. Time responses of ΔP_e (solid line) and ΔP_{e2} (dashed line) to a step of $\Delta\omega$.

changes of the new model transient behaviour in comparison to the old one. In this paper the chosen value is that of $\tau_1 = 30$ s. Responses to the step input of ideal reference model (3) and model (17) are shown in Fig. 12. From Fig. 12 we can see that there is no substantial difference between the two responses in the first few seconds. To make the right hand side in (15) equal to the right hand side in (17) expression for G_1 must be

$$G_1 = -\frac{\tau_1 \left(s + \frac{K}{4H}\right)^2}{(\tau_1 s + 1)} G_r = \frac{2H}{\tau_B} \frac{\left(s + \frac{K}{4H}\right)^2}{\left(s + \frac{1}{\tau_1}\right)\left(s + \frac{1}{\tau_B}\right)} + \frac{1}{R} \frac{\left(s + \frac{K}{4H}\right)^2}{\left(s + \frac{1}{\tau_1}\right)\left(s + \frac{1}{\tau}\right)} G_g G_t = G'_i + G'_m. \quad (18)$$

For values $H = 5$ and $K = 1$, the first term on the right hand side in (18) has a double zero $z_{1/2} = -K/4H = -0.05$ and poles $p_1 = -1/\tau_1 = -0.033$ and $p_2 = -1/\tau_B = -\omega_B = -15$. The zero at -0.05 and the pole at -0.033 are quite slow (and very close to each other) in comparison to the second pole. For this reason they can be cancelled so the first part of transfer function can be simplified to

$$G'_{ii} = \frac{2H}{\tau_B} \frac{\left(s + \frac{K}{4H}\right)}{\left(s + \frac{1}{\tau_B}\right)} = \frac{K}{2} \frac{\left(\frac{4H}{K}s + 1\right)}{(\tau_B s + 1)} = K_1 \frac{\left(\frac{4H}{K}s + 1\right)}{(\tau_B s + 1)}, \quad (19)$$

where $K_1 = K/2$. Regarding the position of its zeros and poles, transfer function G'_{ii} represents transfer function of lead compensator. The second term on the right hand side of (18) has double zero $z_{1/2} = -K/(4H) = -0.05$ and poles $p_1 = -1/\tau_1 = -0.033$ and $p_2 = -1/\tau \approx p_1$. Since poles and zeros of the second term in (18) are very close; for the purposes of transient analysis they can be cancelled as well. This way transfer function of the second term in (18) can be simplified to

$$G'_{mm} = \frac{1}{R} G_g G_t = K_2 G_g G_t. \quad (20)$$

Accordingly, the transfer function G_1 becomes

$$G_1 = K_1 \frac{\left(\frac{4H}{K}s + 1\right)}{(\tau_B s + 1)} + K_2 G_g G_t. \quad (21)$$

Block diagram of the final control law given by (21) is presented in Fig. 4.

IV. SIMULATION RESULTS

Simulation was performed using Matlab and Simulink. A simple electrical power system consisting of two areas, each represented by equivalent generating units with a reheat steam turbine of nominal active power $P_{n1} = P_{n2} = 400$ MW (see Fig. 13), is used for simulation. The areas are connected by a tie line with synchronizing torque coefficient (transmission line constant) $T = 4$. In the first scenario, a reference-GUNRST of nominal active power of $P_{nr} = 200$ MW is connected to the bus of the upper generating unit in Fig. 13. In the second scenario, a VSWG of nominal active power $P_{nw} = 200$ MW is connected instead of reference-GUNRST. The transfer functions of governor and turbine of the generating unit with a reheat steam turbine are as follows [1]:

$$G_{g1} = G_{g2} = \frac{1}{T_G s + 1} \quad (22)$$

$$G_{t1} = G_{t2} = \frac{s F_{HF} T_{RH} + 1}{(T_{CH} s + 1)(T_{RH} s + 1)}. \quad (23)$$

The transfer function of reference-GUNRST governor is the same as transfer function (22). The transfer function of turbine of reference-GUNRST is

$$G_{tr} = \frac{1}{T_{CH} s + 1}. \quad (24)$$

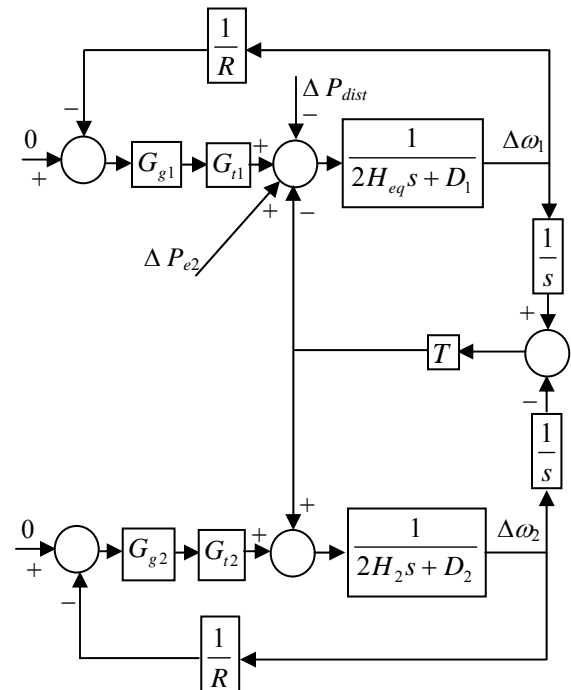


Fig. 13. Model of two area interconnected system with frequency support.

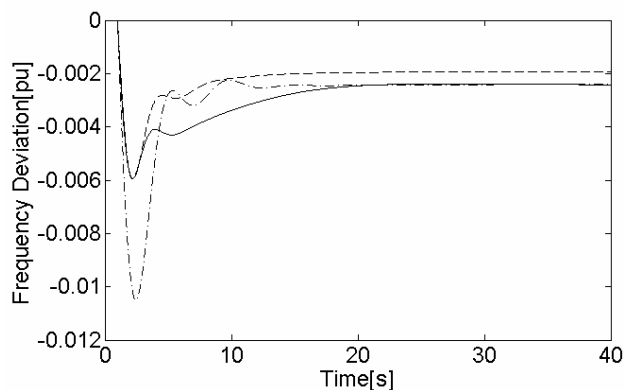


Fig. 14. Frequency response: with support by VSWG (solid line), with support by reference-GUNRST unit (dashed line), and without support (dash dotted line).

Values of parameters in (22), (23), and (24) are given in the Appendix. VSWG mathematical model is identical to that presented in Fig. 9 with added new control signal as shown in Fig. 11. Saturation of signals is not considered. Frequency deviations following a step disturbance of active power $\Delta P_{dist} = 50$ MW (5% of EPS nominal active power), applied on the bus of the first generating unit, are presented in Fig.14. Parameters of VSWG controller used in the simulation are $K = 2$, $T_i = 8H/K = 20$ s, $K_1 = K/2$, and $K_2 = 32$. The value of parameter K_2 is close to value $1/R = 25$. Fig. 14 indicates that the same ROCOF and frequency nadir are achieved by using reference-GUNRST unit and VSWG. Since VSWG that operate at MPPT have no spinning reserve, SSFD has larger value in case of using VSWG than in the case of using reference-GUNRST.

V. CONCLUSIONS AND FUTURE WORK

Due to increased ratio of VSWG penetration in electrical energy generation frequency dynamic response of EPS is worsening. In order to reverse this trend VSWG should “replace” conventional generating units of EPS not only in stationary state but VSWG must contribute to primary frequency control as well. Using the proposed control algorithm it is ensured that in the first seconds after an active power disturbance VSWG “behaves” as the conventional generating unit with the fastest response (GUNRST). Further research in this area should be directed to application of the proposed control algorithm to realistic EPS and combination of the proposed control algorithm and deloading control. Coordination of primary frequency control systems on wind farm and EPS levels should also be researched. Finally, nonlinear analysis and synthesis of VSWG control system could be interesting area for further research.

APPENDIX

Parameters used in simulations.

Main gate servomotor constant: $T_G = 0.2$ s, reheat time constant: $T_{RH} = 7$ s, charging time constant: $T_{CH} = 0.3$ s, droop constant: $R = 0.04$, fraction – HP turbine power: $F_{HP} = 0.3$, inertia constant: $H = H_1 = H_2 = H_w = 5$, load damping: $D_1 = D_2 = 1$, synchronizing torque coefficient (transmission line

constant): $T = 4$, active power base: $P_{base} = P_{n1} = P_{n2} = 400$ MW, nominal grid frequency : $\omega_{base} = 50$ Hz. Equivalent inertia constant of generating unit in the area 1 is calculated as

$$H_{eq} = H_1 + c \frac{P_{nr}}{P_{base}} H, \text{ where } c = 0 \text{ in the case that VSWG is}$$

connected on bus of area 1. In this case $H_{eq} = H_1 = 5$. In the case that GUNRST is connected on bus of area 1 then $c = 1$ and $H_{eq} = 7.5$.

REFERENCES

- [1] P. Kundur, Power System Stability and Control. New York: Mc Graw-Hill, 1993, ch. 11.
- [2] O. Anaya-Lara, N. Jenkins, J. Ekanayake, P. Cartwright, and M. Hughes, Wind Energy Generation – Modeling and Control. West Sussex, U.K.: Wiley, 2009.
- [3] F. M. Hughes, O. Anaya-Lara, N. Jenkins, and G. Strbac, “Control of DFIG-based wind generation for power network support,” IEEE Trans. Power Systems, vol. 20, no. 4, pp. 1958-1966, Nov. 2005.
- [4] J. Morren, S. W. H. de Haan, W. L. Kling, and J. A. Ferreira, “Wind turbines emulating inertia and supporting primary frequency control,” IEEE Trans. Power Systems, vol. 21, no. 1, pp. 433-434, Feb. 2006.
- [5] G. Ramtharan, J. B. Ekanayake, and N. Jenkins, “Frequency support from doubly fed induction generator wind turbines,” IET Renewable Power Generation, vol.1, pp. 3-9, March 2007.
- [6] N. R. Ullah, T. Thiringer, and D. Karlsson, “Temporary primary frequency control support by variable speed wind turbines – potential and applications,” IEEE Trans. Power Systems, vol. 23, no. 2, pp. 601-612, May 2008.
- [7] J. F. Conroy and R. Watson, “Frequency response capability of full converter wind turbine generators in comparison to conventional generation,” IEEE Trans. Power Systems, vol. 23, no. 2, pp. 649-656, May 2008.
- [8] P.-K. Keung, L. Li, H. Banakar, and B. T. Ooi, “Kinetic energy of wind-turbine generators for system frequency support,” IEEE Trans. Power Systems, vol. 24, no.1, pp. 279-287, Feb. 2009.
- [9] J. Duval and B. Meyer, “Frequency behavior of grid with high penetration rate of wind generation,” in Power Tech 2009 Conf., Bucharest, Romania, June 28 – July 2, 2009, pp. 1-6.
- [10] M. Akbari, S. M. Madani, “Participation of DFIG based wind turbines in improving short term frequency regulation,” in Proc. Electrical Engineering (ICEE) 18th Iranian Conf., Isfahan, Iran, May 11-13, 2010, pp. 874-879.
- [11] J. M. Mauricio, A. Marano, A. Gomez-Exposito, and J. L. M. Ramos, “Frequency regulation contribution through variable-speed wind energy conversion systems,” IEEE Trans. Power Systems, vol. 24, no.1, pp. 173-180, Feb. 2009.
- [12] Y.-Z. Sun, Z.-S. Zhang, G.-J. Li, and J. Lin, “Review on frequency control of power systems with wind power penetration,” in Proc. Power System Technology (POWERCON), 2010 International Conf., Hangzhou, China, Oct. 24-28, 2010, pp. 1-8.
- [13] J. J. Grainger and W. D. Stevenson, Power System Analysis. New York: Mc Graw-Hill, 1994.
- [14] H. Knudsen and J. N. Nielsen, “Introduction to the modeling of wind turbines,” in Wind Power in Power Systems, T. Ackermann, Ed. Chichester, U. K.: Wiley, 2005, pp. 525-585.
- [15] N. W. Miller, W. W. Price, and J. C. Sanchez-Gasca, Dynamic Modeling of GE 1.5 and 3.6 Wind Turbine-Generators, GE-Power System Energy Consulting, Tech. Rep. Version 3.0, Oct. 2003.
- [16] N. W. Miller, J. J. Sanchez-Gasca, W. W. Price, and R. W. Delmerico, “Dynamic modeling of GE 1.5 and 3.6 MW wind turbine-generators for stability simulations,” in Proc. IEEE Power Eng. Soc. General Meeting, July 2003, pp 1977-1983.
- [17] T. Ackerman, at all, Wind Power in Power systems – Second Edition. John Wiley & Sons, 2012.
- [18] M. Chinchilla, S. Arnaltes, and J. C. Burgos, “Control of permanent magnet generators applied to variable-speed wind-energy systems connected to the grid,” IEEE Trans. Energy Conversion., vol. 21, no. 1, pp. 130-135, March 2006.

**Creative Commons Attribution License 4.0
(Attribution 4.0 International, CC BY 4.0)**

This article is published under the terms of the Creative Commons Attribution License 4.0

https://creativecommons.org/licenses/by/4.0/deed.en_US